Pull Force and Tail Breaking Force Optimization of the Crescent Bonding Process with Insulated Au Wire

[1]J. Lee, [1]M. Mayer, [1]Y. Zhou and [2]J. Persic

[1]Microjoining Lab, Centre of Advanced Materials Joining, Department of Mechanical and Mechatronics Engineering, University of Waterloo, Waterloo, Canada

[2]Microbonds Inc., Markham, Canada

j75lee@engmail.uwaterloo.ca

Abstract

Strong crescent bond and strong tail bond are crucial for maintaining reliability and bondability of the wire bond and stability of the bonding process, respectively. This study investigates the optimization of tail breaking force and pull force of the crescent bonding process with insulated X-Wire^{TM}. The pull force and the tail breaking force are individually optimized by an iteration method. The results are compared with the results of bare Au wire. Ultrasonic power which is a measure of ultrasonic amplitude, combined with a cleaning stage during bonding plays a significant role in initiating the removal of the insulated layer of X-Wire^{TM} during the crescent bonding process. The pull force and the tail breaking force of insulated X-Wire^{TM} are 91.4 $\pm$ 11.78 mN and 59.15 $\pm$ 5.35 mN, comparable to those of bare Au wire.

Introduction

As the semiconductor industry moves from shrinking die on pad pitch to 3-D packaging solutions [1] to meet the demands of low cost, higher I/O interconnection, and more electrical power for electronic devices, new and disruptive technologies are needed to meet the many challenges in the microelectronics packaging industry.

Insulated bonding wire such as insulated X-Wire^{TM} is a disruptive technology that is gaining more and more momentum [1]. It can improve the flexibility of wire bond design because of its insulating capability, so the wires can touch each other without impairing the device specifications. Longer wires, sagging wires, crossing wires, lower loops, wire sway, and wire sweep are no roadblocks to production anymore and can be acceptable if insulated X-Wire^{TM} is used. During the ball bonding process, the insulation of X-Wire^{TM} is readily removed by the EFO process. Proper parameter settings result in FAB properties comparable to those obtained with bare Au wire.

Standard industry wire bonding equipment using ultrasonic transducers operating at frequencies of 120kHz and greater are typically used to bond bare bonding wire to acceptable pull strength; however, the bonding behavior of insulated X-Wire^{TM} is different from that of bare Au wire in the case of the crescent bond. Without optimization of bond parameters, the insulated wire bond pull strengths are not comparable to bare wire bonds. This study is focused on the crescent bond and its optimization for the case of bonding on Ag plated leadframes.

In addition to the crescent bond, the tail bond is made inside of the capillary as shown in Fig.1 (a). Figure 1 (b) shows the scanning electron microscopy (SEM) image of the crescent bond and the tail bond of Au wire on Au substrate. Tail bonds should be strong enough to hold the wire before the clamp closes. After crescent bonding, the capillary moves up to the tail height where it remains until the clamp closes. It then continues upwards pulling the wire to break it, resulting in a tail of a predefined length. However, if the tail bond is weak, it can lead to non uniform tail length and therefore non uniform free air ball (FAB) formation. Sometimes, the bonder stops before flaming off the tail because the tail bond was weak enough to come loose before the clamp could close, resulting in the wire being blown out from the capillary. This failure is sometimes called “Short tail” or “Tail lift-off”. The frequent occurrence of such process stops reduces the throughput of the wire bond production.

Experimental

ESEC 3088 and 3100 wire bonders were used to optimize the PF and TBF, respectively. A 25µm diameter X-Wire^{TM}

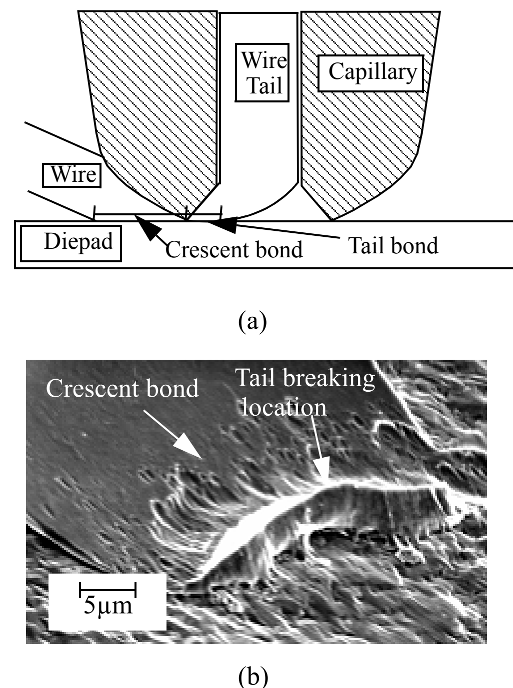

Fig. 1 (a) Illustration of the crescent bond and the tail bond and (b) SEM image showing the crescent bond.

available from Microbonds, Markham, Canada, is used for bonding process. A Au wire with the same diameter is used for comparison. The wires are bonded on PLCC 44 leadframes with 8μm thick Ag metallization The capillary used has tip, chamfer and hole diameters of 100μm, 51μm, and, 35μm, respectively.

Crescent bond optimization

Ball - wedge - wedge (BWW) bonds as shown in Fig. 2 are made at the 3088 bonder. The loops are directed perpendicular to the ultrasonic direction. The bonding temperature (T) and the bonding time (BT) are 220°C and 25ms. The ultrasonic power (USP), impact force (IF), and bonding force (BF) are varied to obtain optimum parameters. An iterative optimization method [3] is used to optimize the PF. The tail pull force (TPF) measurement is conducted with commercial pull tester at the last iteration. A total of 15 pull test measurements are conducted at each bonding parameter combination. In order to confirm the PF at the optimized parameter, 100 test bonds are made on 5 diepads from 5 different leadframes. Number 61 - 80 bonds are pulled from each diepad. In total, 100 bonds are pulled at the optimized parameter and the results are compared with those obtained with bare Au wire. The pull speed is 200μm/s. Figure 3. shows the location of the PF and the TPF measurements indicated by A and B, respectively.

In-situ tail breaking force optimization

In-situ tail breaking force measurement method described in [3, 4] is used to optimize the TBF. Using iterative method [3], the TBF is optimized and the effects of bonding parameters are investigated. A total of 16 measurements at each bonding parameter combination are conducted. To confirm the TBF results at the optimized parameter, a total of 160 measurements

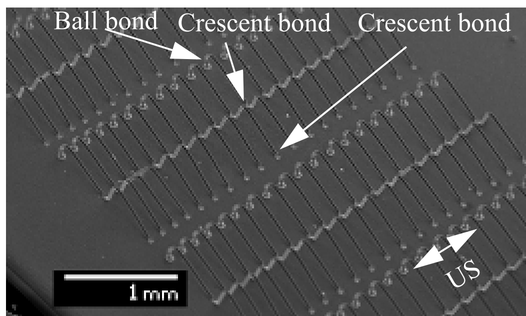

Fig. 2 BWW bonding diagram to optimize the PF of the crescent bond.

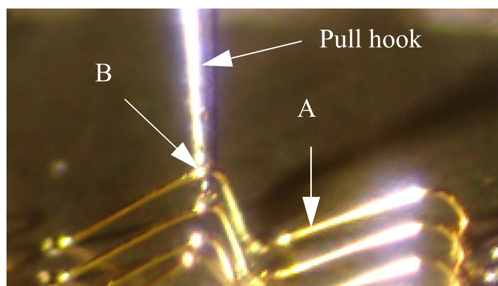

Fig. 3 The TPF set up with commercial pull tester.

are conducted and the results are compared with those obtained with bare Au wire. In order to investigate the effect of USP on the removal of insulated layer of X-Wire^{TM}, the fracture surface on the diepad and the wire after pull test is observed with SEM.

Results and discussion

Crescent bond pull force optimization

The starting parameters for optimization by iteration are IF of 750mN and BF of 350mN. The USP is varied from 5% to 95% to obtain the highest PF. The unit "%" is used for the USP parameter, where 1% is equivalent to a peak to peak vibration amplitude of 26.6nm measured at the center of the transducer tip. After the optimization of the USP, consequently the IF and the BF are optimized until the maximum PF is obtained. The iteration results are summarized in Table 1. The maximum PF of 65.16 ± 7.4mN is obtained at USP, IF, and BF of 15%, 500mN, and 500mN, respectively.

Figures 4 (a) - (c) show the PF results versus USP, IF, and BF, respectively, with optimized values for the other parameters. The wire is bondable for the whole USP range (5 - 95 %) of the bonder. IF and BF are up to 2000mN and 1000mN, respectively. For BF lower than 300mN, bond lift-off occurs. The fracture during the pull test occurs at the interface between the wire and the diepad at BF between 300mN and 450mN. With BF higher than 500mN, the fracture occurs at the wire, resulting in strong bonds. The PF does not significantly change as the BF increases further.

In order to confirm the PF results, a total of 100 bonds are made with the optimized parameters and the results are compared with those obtained with bare Au wire. Figure 5 shows the PF comparison results between X-Wire^{TM} and bare Au wire at the optimized parameters. The optimized parameters are USP of 15%, IF of 500mN, and BF of 500mN. Comparing the PFs between at the last iteration in Table 1and at the optimized parameters in Fig. 5, it can be seen that the PFs at the same parameters are different. The effect of diepad variation on the PF is investigated with 6 different diepad and the results are shown in Fig. 6.

In order to eliminate the effect of the diepad variation, 5 die pads randomly chosen from 10 leadframes are used for the bonding process. The average pull forces of X-Wire^{TM} and bare Au wire are 71.47 ± 7.97mN and 88.93 ± 8.50mN, respectively, which is about 80% of the PF of bare Au wire.

A cleaning stage is inserted to the bonding parameter profile before the bonding stage to improve an insulation removal

Table 1. Summary of the crescent bond PF of X-Wire^{TM} by iteration

Iteration	USP (%)	IF (mN)	BF (mN)	Av. PF (mN)	σ (mN)
1	30	700	400	61.6	9.51
2	15	500	500	65.16	7.4
3	15	500	500	64.74	7.3

and the pull force of the X-Wire^{TM}. The original and modified profiles are shown in Figs. 7 (a) and (b), respectively. A larger IF is applied in a cleaning stage to produce a larger deformation of the crescent bond and therefore the large interfacial contact area. The cleaning stage is introduced toward to ball direction after the impact. During the cleaning stage, the BF is reduced by 50% to avoid bonding and facilitate the shifting motion. A total shift distance during the cleaning is 20μm. This cleaning stage is followed by a bonding stage with the original parameters. With this modified process, the average pull force is comparable with that of obtained with bare Au wire as shown in Fig. 5.

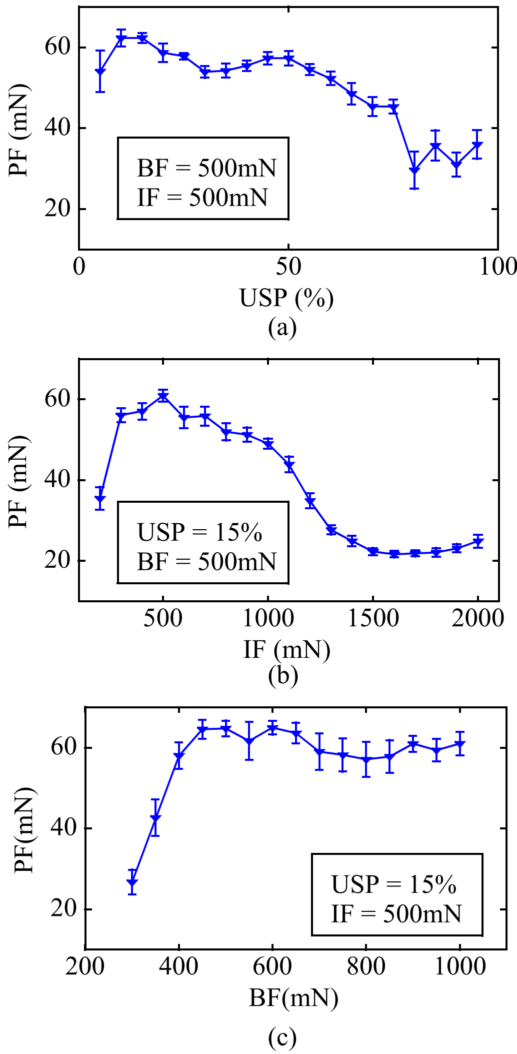

Fig. 4 PF results vs. (a) USP, (b) IF, and (c) BF. T = 220°C, BT = 25ms

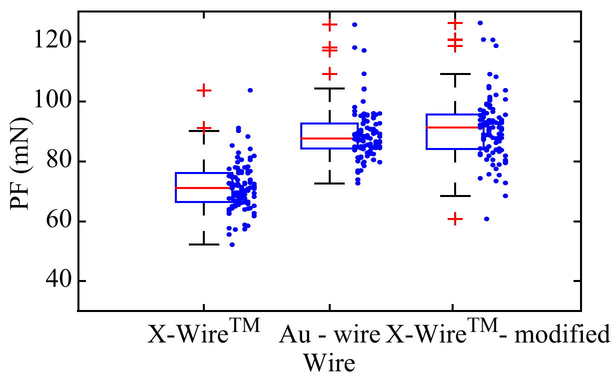

Fig. 5 Crescent bond pull force comparison at the optimized parameters and modified bonding parameter.

Tail pull force measurement

During the optimization process by iteration, EFO errors (or short tail) are observed as shown in Fig. 8. This is due to premature tail break [5]. This may lead to a decrease in the stability of the crescent bonding process. Thus, the TPF is measured at various USP to investigate the effect of USP on the TPF. During the TPF measurement, the tail bond made at the first crescent bond breaks as indicated by c in Fig. 9. Figure 10 shows the tail pull force results at the third iteration of the crescent bond optimization. The TPF increases as the USP increases from 10% to 20%. It remains constant up to USP of 45% and then decreases. The maximum TPF obtained is

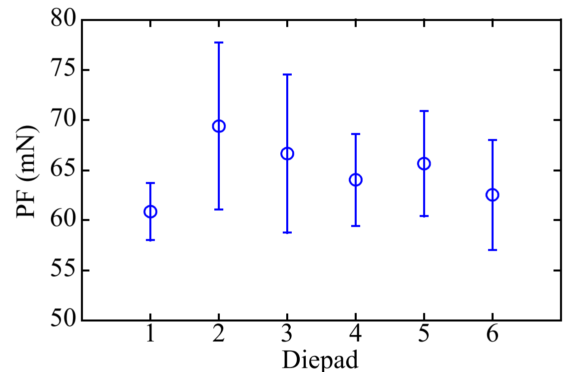

Fig. 6 Average PF change versus diepads.

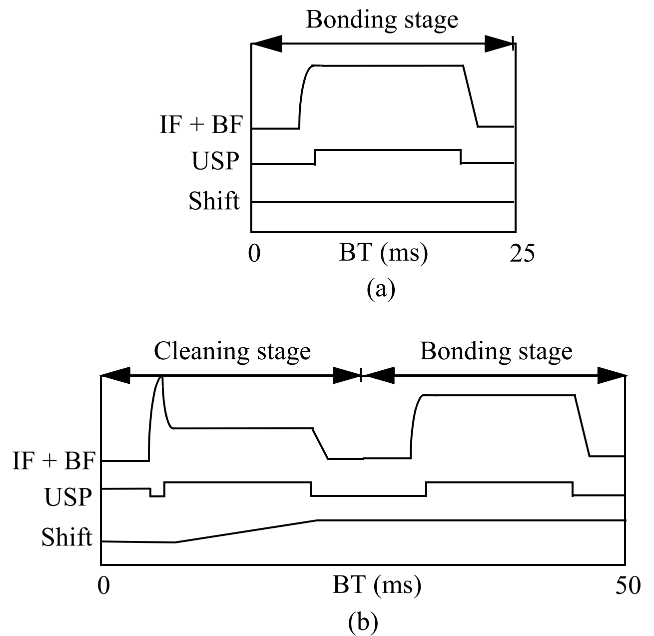

Fig. 7 Crescent bond process parameter profiles. (a) original and (b) modified

46.71mN at USP of 45%. The TPF at the optimized parameter is 30.95mN.

In-situ tail breaking force optimization

The TPF test with commercial pull tester is time consuming. Furthermore, during wire looping to the second crescent shown in Fig. 3, the tail bond may be weaken due to the friction between the capillary and the wire and the bonding during the second looping process. In order to obtain an accurate tail bond strength, the in-situ tail breaking force (TBF) measurement method [4] is used.

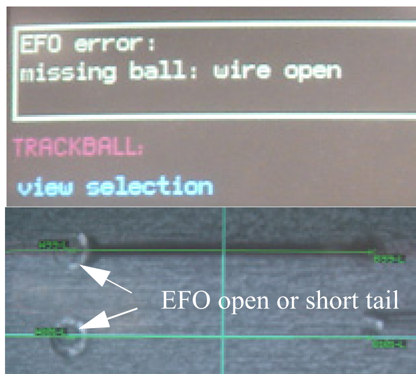

Fig. 8 Short tail error message displayed in the ESEC 3088 bonding machine.

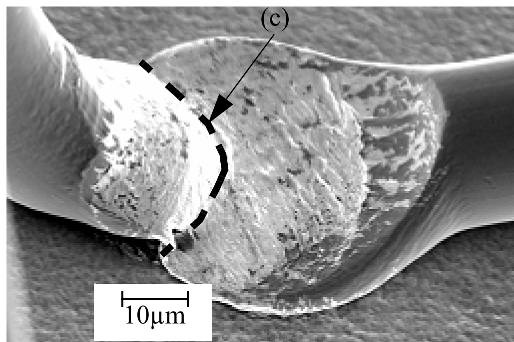

Fig. 9 SEM image showing the first (middle) crescent bond made during BWW bonding process.

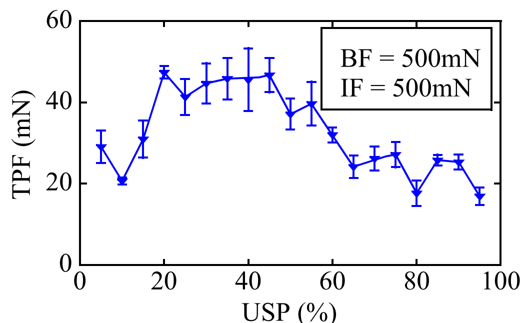

Fig. 10 Tail pull forces measured at third iteration of the crescent bond optimization at various USP.

Figure 11 shows an example measurement of the TBF signal measured during X-Wire^{TM} crescent bond process. The signal increases before the tail breaks as the wire tension increases. After it reaches a maximum value, the signal suddenly drops to zero indicating tail breaking. With the online TBF measurement method, the TBF of Au X-Wire^{TM} is maximized using an iteration method the results of which are summarized in Table 2. Figures 12 (a) - (c) show the 3rd iteration (last iteration) results at various bonding parameters. The error (ε) is calculated with the formula below

$$\varepsilon = \frac{\sigma}{\sqrt{(n-1)}}$$

n is the sample size.

The TBF is 42 mN at a USP of 28%. Sharp increase of the TBF is observed as USP increases from 28% to 38%. After USP higher than 38%, it increases slowly and then stays constants as shown in Fig. 12 (a). With IF increase from 300mN to 1150mN, the TBF does not change. It decreases as IF increases further as shown in Fig. 12 (b.). The TBF does not change as BF increases from 300mN to 700mN. It increases as BF increases from 700mN to 900mN and then decreases. The maximum TBF, 60mN, obtained with X-Wire^{TM} is comparable to that obtained with bare Au wire.

In order to obtain a reliable comparison, a confirmation run with 160 measurements with the optimized parameters was conducted. The results of bare Au wire and X-Wire^{TM} are shown in Fig. 13.

Effect of ultrasonic power on the tail breaking force and the pull force

It is clear from Figs. 14 (a) - (c) that Au residues remain on the tail bond region after the crescent bond. The circle of the images is defined to be the capillary hole. The tail bond forms not only at the area where the wire is pinched by the capillary chamfer and the die pad [5], but also inside of capillary hole.

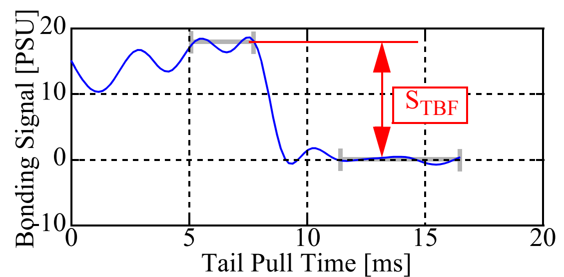

Fig. 11 Example measurement of TBF signal

Table 2. Summary of the TBF of X-Wire^{TM} by iteration

Iteration	USP (%)	IF (mN)	BF (mN)	Av. PF (mN)	σ (mN)
1	44	900	650	60.18	5.8
2	58	750	800	61.25	5.62
3	58	800	800	62.72	5.6

As USP increases, the area pinched by the capillary chamfer and the die pad remains larger after the pull test as indicated by A and B in Figs. 14 (b) and (c), respectively.

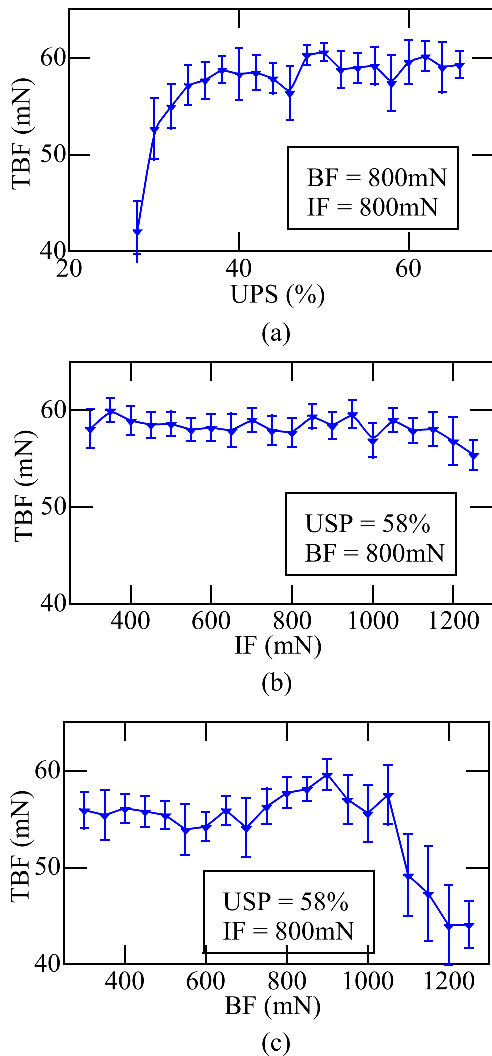

Fig. 12 TBF results of 3rd iteration of X-Wire™. (a) USP, (b) IF, and (c) BF.

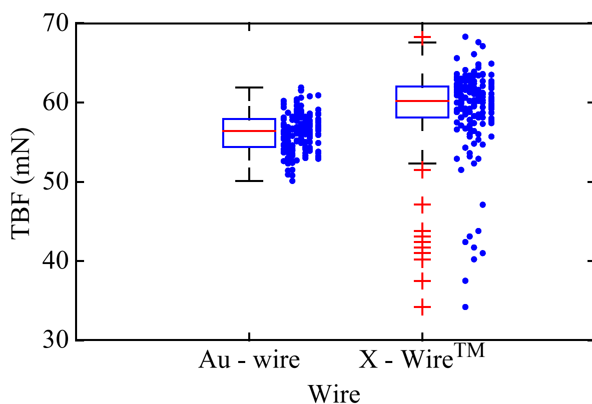

Fig. 13 TBF comparison results at the optimized parameters.

To study the influence of USP on the PF, the fracture surfaces of the diepad and of the wire after wire pull test are investigated with SEM. Back scattered electron (BSE) microscopy is employed to obtain better contrast depending on the materials. Figures 14 (a) - (c) show the BSE images at various USP. The bonds are only formed at the periphery of the crescent bond at USP of 40% as shown in Fig. 14 (a). As USP increases to 52%, the bond area increases and it increases to the center of the crescent bond as shown in Fig. 14 (b). Further

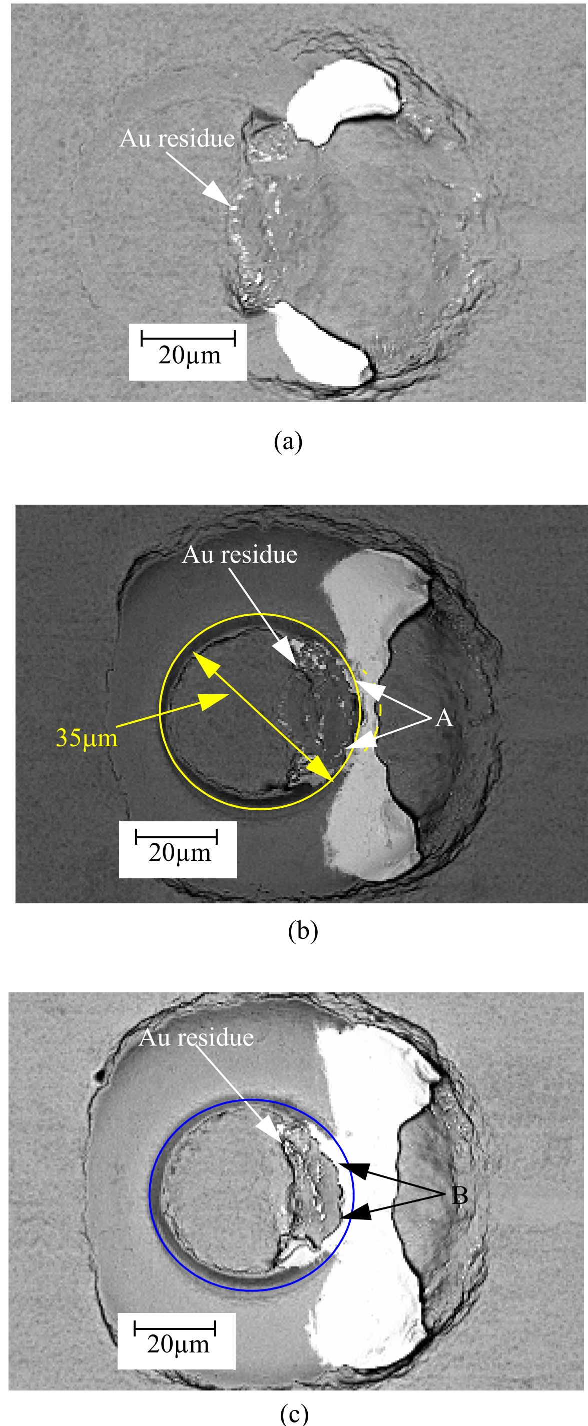

Fig. 14 BSE images of fracture surface on the die at various USP. (a) 50%, (b) 52%, and (c) 60%

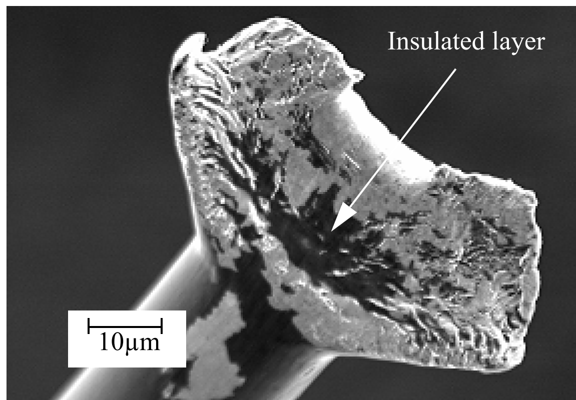

(a)

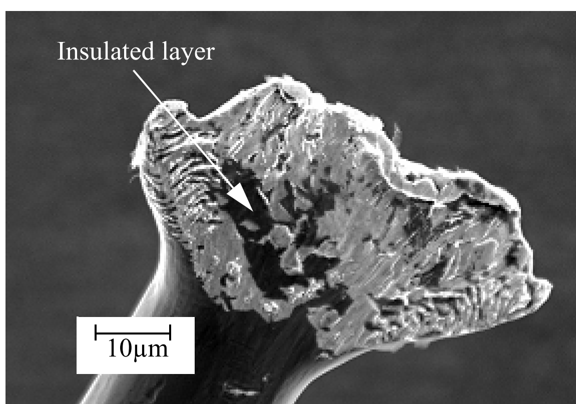

(b)

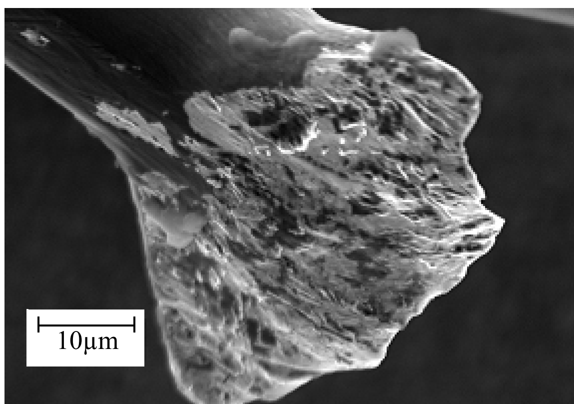

(c)

Fig. 15 SE images of fracture surface on the wire at various USP. (a) 40%, (b) 52%, and (c) 60%

increase of USP to 69% results in increasing area of the crescent bond as shown in Fig. 14 (c), which well agrees with the result reported by [6, 7].

Figures 15 (a) - (c) show secondary electron (SE) images at various USP. It is clear that the remaining insulated layer decreases as US increases. The remaining area covered by insulation at 40% of USP is about 350μm^2. It decreases to 180μm^2 as USP increases to 52%. When US reaches to 40%, the insulated layer is completely removed. It is clear from the observation made in this study that USP plays important roles not only in increasing bonded area, resulting in higher PF, but also in initiating the removal of the insulated layer.

Conclusion

The second bond of insulated X-Wire^{TM} are studied. Standard bond parameters used to bond bare wire on wire bonders, typically equipped with ultrasonic transducers operating at frequencies of 120kHz and greater, are not sufficient to bond insulated wire to the equivalent pull strengths. Both the crescent bond pull force and the tail breaking force depend on the bonding parameters which can be readily optimized for X-Wire^{TM}. In this study it was found that impact force does not affect the tail breaking force compared to the other parameters. Ultrasonic power, combined with a cleaning stage during bonding, can play a significant role in crescent bond formation and initiating the insulation removal of insulated X-Wire^{TM}. The modified bonding process improves the average pull force of X-Wire^{TM}. The average pull force and the tail breaking force obtained with X-Wire^{TM} are comparable to those obtained with Au wire.

Acknowledgement

This work is supported by Microbonds Inc. (Markham, Canada), NSERC, AuTEK, and OCE (all from Canada). The technical help of Oerlikon ESEC is gratefully acknowledged (Swizerland, USA, and Singapore).

Reference

[1] "Assmbly and Packaging" ITRS 2006 update, pp. 1-19

[2] K. S. Goh, Z. W. Zhong,"Two capillary solutions for ultra-fine-pitch wire bonding and insulated wire bonding", *Microelectronic Eng*. Vol. 84, No. 2 (2007), pp. 362-367.

[3] J. Lee, M. Mayer, Y. Zhou, S. J. Hong, "Iterative Optimization of Tail Breaking Force of 1mil Wire Thermosonic Ball Bonding Processes and the Influence of Plasma Cleaning" *in press in Microelectronics Journal*.

[4] J. Lee, M. Mayer, Y. Zhou, S. J. Hong, and S. M. Lee, "Tail breaking force in thermosonic wire bonding with novel bonding wires", *Proc IWJC-Korea*, Seoul, Korea, 2007, pp. 271.

[5] J. Beleran, A. Turiano, D. M. Calpito, D. Stephan, Saraswati, F. Wulff, and C. Breach " Tail Pull Strength of Cu wire on Gold and Silver-plated Bonding leads" *Proc. SEMICON*, Singapore (2005), pp. 1-8.

[6] Y. N. Zhou, X. Li, N. J. Noolu,"A footprint study of bond initiation in gold wire crescent bonding" *IEEE Trans. Comp. Packag. Technol*., Vol 28, No. 4 (2005), pp. 810-816.

[7] M. Weissenfelt, P. Collander, E. Jarvinen, T. Laurinolli, "A practical method for evaluating and adjusting ultrasonic wire bonding process", *Proc. 29th Electro. Comp. Conf.* Cherry Hill, N. J. USA (1979), pp. 309-314.